Model-Based Design of a Cascade Control for Loop Heat Pipes

Modellbasierter Entwurf einer Kaskadenregelung für Loop Heat Pipes

Thomas Gellrich and Soeren Hohmann

Karlsruhe Institute of Technology, Institute of Control Systems,
Kaiserstr. 12, Karlsruhe, e-mail: thomas.gellrich@kit.edu

Abstract — This paper presents the model-based design of a cascade control for loop heat pipes (LHPs). LHPs are passive, two-phase heat transport systems, which have been developed for the thermal control of aerospace systems. Through evaporation and condensation, the working fluid inside the loop transports large amounts of heat from the heat source to the heat sink. For a constant temperature near the heat source, the LHP itself must be controlled. It is common practice to control the temperature of the compensation chamber (CC), which governs the evaporator temperature of the LHP as the nearest measurable LHP temperature to the heat source. However, changes of the dissipated heat at the heat source and of the temperature at the heat sink disturb the evaporator temperature when controlling the CC temperature at a fixed setpoint temperature. For this reason, a cascade control is designed based on a nonlinear dynamical model of the LHP in this work. Thus, not only the CC temperature, but also the evaporator temperature is controlled in two control loops. In addition, the influences on the evaporator temperature during LHP operation are decreased compared to the direct control of the evaporator temperature.

Zusammenfassung — Diese Arbeit präsentiert den modellbasierten Entwurf einer Kaskadenregelung für Loop Heat Pipes (LHPs). LHPs sind passive, zweiphasige Wärmetransportsysteme, welche für die Thermalkontrolle von Luft- und Raumfahrtsystemen entwickelt wurden. Durch Verdampfung und Kondensation transportiert das Arbeitsmedium im Kreislauf große Wärmemengen von der Wärmequelle zur Wärmesenke. Für eine konstante Temperatur an der Wärmequelle muss die LHP selbst geregelt werden. Typischerweise wird die Temperatur der Kompensationskammer (CC) geregelt, die die Verdampfertemperatur der LHP als die nächstgelegene, messbare Temperatur zur Wärmequelle bestimmt. Jedoch stören die Änderungen der dissipierten Wärme der Wärmequelle und der Senkentemperatur die Verdampfertemperatur, wenn die CC-Temperatur auf eine feste Solltemperatur geregelt wird. Aus diesem Grund wird in dieser Arbeit eine Kaskadenregelung auf Basis eines nichtlinearen, dynamischen Modells der LHP entworfen. Dadurch können in zwei Regelungsschleifen nicht nur die CC-Temperatur, sondern auch die Verdampfertemperatur geregelt werden. Des Weiteren werden die Einflüsse auf die Verdampfertemperatur während des Betriebs der LHP im Vergleich zur direkten Regelung der Verdampfertemperatur verringert.

I. Introduction

Loop heat pipes (LHPs) are widely used for the thermal control of satellite components [1]. Their working principle is based on capillary forces in a primary wick instead of mechanical pumping forces. Besides the passive driving force for the mass flow, the two-phase system reaches a high thermal conductance at a small temperature difference between the heat source, which is the electronics in a satellite component, and the heat sink through the evaporation and condensation of the working fluid. The transient mass distribution in the entire loop is balanced by the two-phase compensation chamber (CC). In addition, this CC supplies the primary wick with liquid through the secondary wick for a continuous heat transport. For a more detailed description of the LHP working principle, the reader is referred to [2]. To keep the temperature of the heat source in a small temperature corridor during LHP operation, the LHP operating temperature itself must be controlled against changing operating conditions. First, the temperature of the heat sink, e.g. the radiator of the satellite, at the LHP condenser changes due to the variable insolation of the satellite in space. Second, the amount of dissipated heat of the electronics near the LHP evaporator depends on their operating status. A widely used control strategy is the application of a control heater on the balancing CC [3]. For the control heater, two-point-controllers [4], [5], [6] and proportional-integral-derivative (PID) controllers [5], [6] for different directly controlled LHP temperatures have been designed heuristically and tested experimentally. However, the common method of maintaining the LHP operating temperature in a small corridor is to control the CC temperature [3]. This method yields the most stable temperatures and the least risk for temperature oscillations at low powers compared to directly controlling the evaporator temperature or the heat source temperature [6]. Due to the recent development of an dynamical control model of the LHP in [7] for the model-based control design for the control heater, more sophisticated control algorithms can be designed to improve the overall thermal control performance of the LHP. Current model-based controllers focus on the sole control of the CC temperature [8], [9]. Hence, an adequate model-based control design for the evaporator temperature of the LHP should improve the temperature control of the electronics, which is the main goal of the thermal control of satellite components with LHPs.

In this paper, a cascade control based on linear feedback controllers for the control heater is designed based on the recently developed nonlinear dynamical model in [7]. Instead of directly controlling the evaporator temperature as the nearest measurable LHP temperature to the heat source, the inner loop of the cascade control still controls the CC temperature, while the outer loop controls the evaporator temperature. By separating the system's dynamics into two parts for the two cascaded control loops, the overall control performance is improved compared to the direct control in a single control loop. Another advantage of the cascade control structure is the simple extension of the single LHP control loops in the literature based on the CC temperature with another outer control loop based on the evaporator temperature to preserve their benefits in the inner control loop. The additional lightweight temperature sensor on the evaporator is often already integrated in the LHP system for monitoring the interface between the heat transport system and the heat source.

In Section II, the dynamical LHP model is described. After the design of the cascade control in Section III, the numerical results of the introduced cascade control in comparison with the direct control are shown in Section IV, followed by the conclusions in Section V.

II. Dynamical LHP Model

The nonlinear dynamical LHP model developed in [7] is taken as the control model for the subsequent cascade control design:

$$\dot{\boldsymbol{x}}(t) = \boldsymbol{f}\left(\boldsymbol{x}(t), u(t), \boldsymbol{d}(t)\right), \quad (1a)$$
$$\boldsymbol{y}(t) = \boldsymbol{x}(t), \quad (1b)$$

with $\boldsymbol{x}(t) = [T_{cc}(t), T_{ev}(t), T_{co}(t)]^\top$, $u(t) = \dot{Q}_{cc}(t)$, and $\boldsymbol{d}(t) = [\dot{Q}_{ev}(t), T_{sk}(t)]^\top$. The nonlinear state-space model (1) contains the CC temperature $T_{cc}(t)$, the evaporator temperature $T_{ev}(t)$, and the condenser temperature $T_{co}(t)$ as state variables $x_1(t), ..., x_3(t)$ in $\boldsymbol{x}(t)$. These state variables correspond to the mean temperatures in the colored subsystems depicted in the schematic of the LHP in Fig. 1. Furthermore, the input variable $u(t)$ describes the heat input $\dot{Q}_{cc}(t)$ by the control heater on the CC. Finally, the external influences on the LHP by the heat source and the heat sink are included in $\boldsymbol{d}(t)$ as disturbance variables $\dot{Q}_{ev}(t)$, the heat flow to the evaporator, and $T_{sk}(t)$, the temperature of the heat sink. All three state variables are measurable outputs $y_1(t), ..., y_3(t)$ of the system and form the output vector $\boldsymbol{y}(t)$.

The nonlinear differential equations of the LHP state-space model (1) are defined as follows (In order to ease

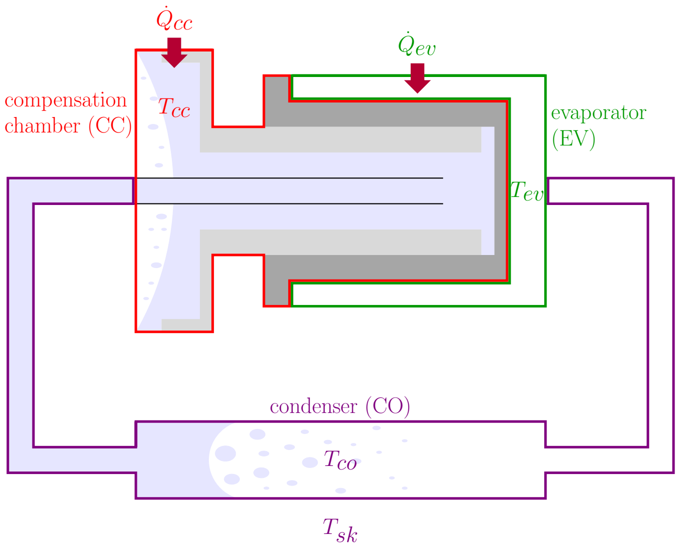

Fig. 1. Schematic of the LHP (cf. [2])

notation, time dependencies are dropped):

$$f_1 = \frac{1}{C_{cc}} \cdot \left(\dot{m} \cdot \bar{c}_p^l \cdot (T_{co} - T_{cc}) + \dot{Q}_{cc} + \frac{1}{R_{lk}} \cdot (T_{ev} - T_{cc}) \right), \quad (2)$$

$$f_2 = \frac{1}{C_{ev}} \cdot \left(\dot{m} \cdot \left(\bar{c}_p^l \cdot (T_{cc} - T_{ev}) - \Delta h_{ev}^v\right) + \dot{Q}_{ev} - \frac{1}{R_{lk}} \cdot (T_{ev} - T_{cc}) \right), \quad (3)$$

$$f_3 = \frac{1}{C_{co}} \cdot \left(\dot{m} \cdot \left(\bar{c}_p^l \cdot (T_{ev} - T_{co}) + \Delta h_{ev}^v\right) - \frac{1}{R_{co}} \cdot \left(\frac{T_{ev} + T_{co}}{2} - T_{sk} \right) \right), \quad (4)$$

with the lumped thermal capacities C_{cc}, C_{ev}, and C_{co} of the corresponding subsystems, $\bar{c}_p^l$ being the mean specific isobaric heat capacity of the respective liquid phase, Δh_{ev}^v being the specific heat of evaporation, and $\dot{m}$ being the mass flow rate of the working fluid. The parameters R_{lk} and R_{co} correspond to the thermal resistances of the heat flow from the evaporator to the CC as part of the heat input $\dot{Q}_{ev}(t)$ and of the heat flow from the condenser to the heat sink, respectively. The parameters are determined in a chosen operating point, where the system reaches a steady state, as described in [7].

III. Model-Based Cascade Control Design

The structure of the LHP cascade control is presented in Fig. 2.

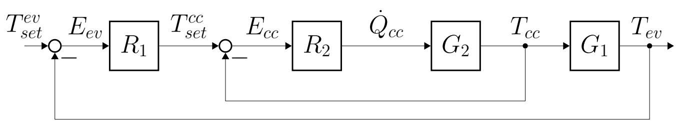

Fig. 2. Cascade control of the LHP

As depicted in Fig. 2, the total LHP system is subdivided into two single-input-single-output (SISO) subsystems for both cascaded control loops. These SISO subsystems are described by transfer functions in the Laplace domain with the complex variable s. For the model-based design of the two cascaded linear feedback controllers $R_1(s)$ and $R_2(s)$, the corresponding subsystems $G_1(s)$ and $G_2(s)$ are derived from the nonlinear LHP state-space model (1).

At first, the nonlinear LHP state-space model (1) is linearized at the chosen operating point, which yields the following linear LHP state-space model:

$$\Delta\dot{\boldsymbol{x}}(t) = \boldsymbol{A}_{lin} \cdot \Delta\boldsymbol{x}(t) + \boldsymbol{b}_{lin} \cdot \Delta u(t) + \boldsymbol{E}_{lin} \cdot \Delta\boldsymbol{d}(t), \quad (5a)$$
$$\Delta\boldsymbol{y}(t) = \boldsymbol{C}_{lin} \cdot \Delta\boldsymbol{x}(t), \quad (5b)$$

with $\Delta\boldsymbol{x}(t) = [\Delta T_{cc}(t), \Delta T_{ev}(t), \Delta T_{co}(t)]^\top$, $\Delta u(t) = \Delta\dot{Q}_{cc}(t)$, and $\Delta\boldsymbol{d}(t) = [\Delta\dot{Q}_{ev}(t), \Delta T_{sk}(t)]^\top$. The matrices in (5) are defined as

$$\boldsymbol{A}_{lin} = \begin{bmatrix} -\mathcal{A} & \frac{1}{C_{cc}R_{lk}} & \frac{1}{C_{cc}}\left(\bar{c}_p^l \dot{m}\right) \\ \mathcal{B} & -\mathcal{B} & 0 \\ 0 & \mathcal{C} & -\frac{1}{C_{co}}\left(\bar{c}_p^l \dot{m} + \frac{1}{2R_{co}}\right) \end{bmatrix}, \quad (6)$$

$$\boldsymbol{b}_{lin} = \begin{bmatrix} \frac{1}{C_{cc}} \\ 0 \\ 0 \end{bmatrix}, \quad (7)$$

$$\boldsymbol{E}_{lin} = \begin{bmatrix} 0 & 0 \\ \frac{1}{C_{ev}} & 0 \\ 0 & \frac{1}{C_{co}R_{co}} \end{bmatrix}, \quad (8)$$

$$\boldsymbol{C}_{lin} = \begin{bmatrix} 1 & 0 & 0 \\ 0 & 1 & 0 \\ 0 & 0 & 1 \end{bmatrix}, \quad (9)$$

with the substitute parameters

$$\mathcal{A} = \frac{1}{C_{cc}}\left(\bar{c}_p^l \dot{m} + \frac{1}{R_{lk}}\right), \quad (10)$$

$$\mathcal{B} = \frac{1}{C_{ev}}\left(\bar{c}_p^l \dot{m} + \frac{1}{R_{lk}}\right), \quad (11)$$

$$\mathcal{C} = \frac{1}{C_{co}}\left(\bar{c}_p^l \dot{m} - \frac{1}{2R_{co}}\right). \quad (12)$$

The linearized LHP state-space model (5) is converted by the Laplace transformation into the transfer functions $G_1(s)$ and $G_2(s)$ of the LHP subsystems in both control loops as follows:

$$G_1(s) = \frac{\Delta T_{ev}(s)}{\Delta T_{cc}(s)} = \frac{\mathcal{B}}{s+\mathcal{B}}, \quad (13)$$

$$G_2(s) = \frac{\Delta T_{cc}(s)}{\Delta\dot{Q}_{cc}(s)} = \begin{bmatrix} 1 & 0 & 0 \end{bmatrix} \cdot (s \cdot \boldsymbol{I} - \boldsymbol{A}_{lin})^{-1} \cdot \boldsymbol{b}_{lin}. \quad (14)$$

First, a feedback controller $R_2(s)$ for the inner control loop is designed according to the transfer function $G_2(s)$ in (14). Then, the inner control loop

$$G_{c1}(s) = \frac{R_2(s)G_2(s)}{1 + R_2(s)G_2(s)} \quad (15)$$

is combined with the transfer function $G_1(s)$ in (13) to form the transfer function

$$G_{c2}(s) = G_{c1}(s) \cdot G_1(s), \quad (16)$$

of the controlled subsystem for the second feedback controller $R_1(s)$ in the outer loop.

The combination of a P and a PI controller is commonly used in the industry for its good performance [10]. For the stationary accuracy of the entire cascade control loop, an integral part in one of the controllers is sufficient [11]. Thus, the transfer functions of both controllers are given as

$$R_1(s) = \frac{\Delta T_{set}^{cc}(s)}{\Delta E_{ev}(s)} = K_{p1} \cdot \frac{1 + T_1 s}{s}, \quad (17)$$

$$R_2(s) = \frac{\Delta\dot{Q}_{cc}(s)}{\Delta E_{cc}(s)} = K_{p2}. \quad (18)$$

The three controller parameters K_{p1}, T_1, and K_{p2} in (17) and (18) can be calculated with the robust response time algorithm in MATLAB (see [12]). With sufficient phase margins and limited robust response times for both controllers, the stability of the control loop and a continuous heat transfer are ensured, since the self-sufficient LHP working principle limits the maximal CC temperature gradient. For improved stability characteristics of the overall cascade control, the dynamics of the inner control loop should be faster than the dynamics of the outer control loop [11], i.e. a smaller robust response time of the inner control loop.

IV. Numerical Results

The validation of the proposed cascade control for the temperature control of LHPs is performed with the experimentally validated numerical LHP simulation of [13]. This simulation, which was already adapted and used for controller validation in [9], provides a safe test environment for LHP controllers based on the variation of the measurable LHP temperatures by a control heater. The following operating point (*op*) is chosen, where the LHP reaches steady-state conditions at the desired setpoint temperature $T_{set}^{ev} = 28.58\,°\text{C}$. In the operating point, the model parameters are determined, and the nonlinear LHP state-space model (1) is linearized:

TABLE I. Values of the state variables, input variables, and model parameters in the chosen operating point

operating point	model parameter
$\dot{Q}_{cc}^{op} = 4.653\,\text{W}$	$C_{cc} = 12.00\,\text{J}\,\text{K}^{-1}$
$\dot{Q}_{ev}^{op} = 60.00\,\text{W}$	$C_{ev} = 3.000\,\text{J}\,\text{K}^{-1}$
$T_{sk}^{op} = 0.000\,°\text{C}$	$C_{co} = 9.000\,\text{J}\,\text{K}^{-1}$
$T_{cc}^{op} = 26.86\,°\text{C}$	$R_{lk} = 1.004\,\text{K}\,\text{W}^{-1}$
$T_{ev}^{op} = 28.58\,°\text{C}$	$\dot{m} = 50.32\,\text{mg}\,\text{s}^{-1}$
$T_{co}^{op} = 0.000\,°\text{C}$	$R_{co} = 0.221\,\text{K}\,\text{W}^{-1}$

Following the procedure in Sec. 3, the three controller parameters are determined with a phase margin of 60.00° and a robust response time of 14.00 s and 18.62 s as

$$K_{p1} = 0.153\,\text{s}^{-1},\ T_1 = 2.556\,\text{s},\ K_{p2} = 1.960\,\text{W}\,\text{K}^{-1}.$$

For the comparison of the relevant disturbance responses of the introduced cascade control loop in Fig. 2 and a direct feedback control loop of the evaporator temperature, a PI controller $R_3(s)$ is designed based on the transfer function $G_3(s)$ of the total evaporator system:

$$G_3(s) = \frac{\Delta T_{ev}(s)}{\Delta \dot{Q}_{cc}(s)} = \begin{bmatrix} 0 & 1 & 0 \end{bmatrix} \cdot (s \cdot \boldsymbol{I} - \boldsymbol{A}_{lin})^{-1} \cdot \boldsymbol{b}_{lin}. \quad (19)$$

Accordingly, the transfer function $R_3(s)$ of the corresponding PI controller is given by

$$R_3(s) = \frac{\Delta \dot{Q}_{cc}(s)}{\Delta E_{ev}(s)} = K_{p3} \cdot \frac{1 + T_3 s}{s}, \quad (20)$$

with the controller parameters

$$K_{p3} = 0.089\,\mathrm{W\,K^{-1}\,s^{-1}},\ T_3 = 14.55\,\mathrm{s}$$

at a phase margin of 60.00° and a robust response time of 18.73 s.

The performance of the presented cascade control (dashed red) in comparison with the performance of the direct controller (dotted green) for a typical LHP disturbance profile is depicted in Fig. 3.

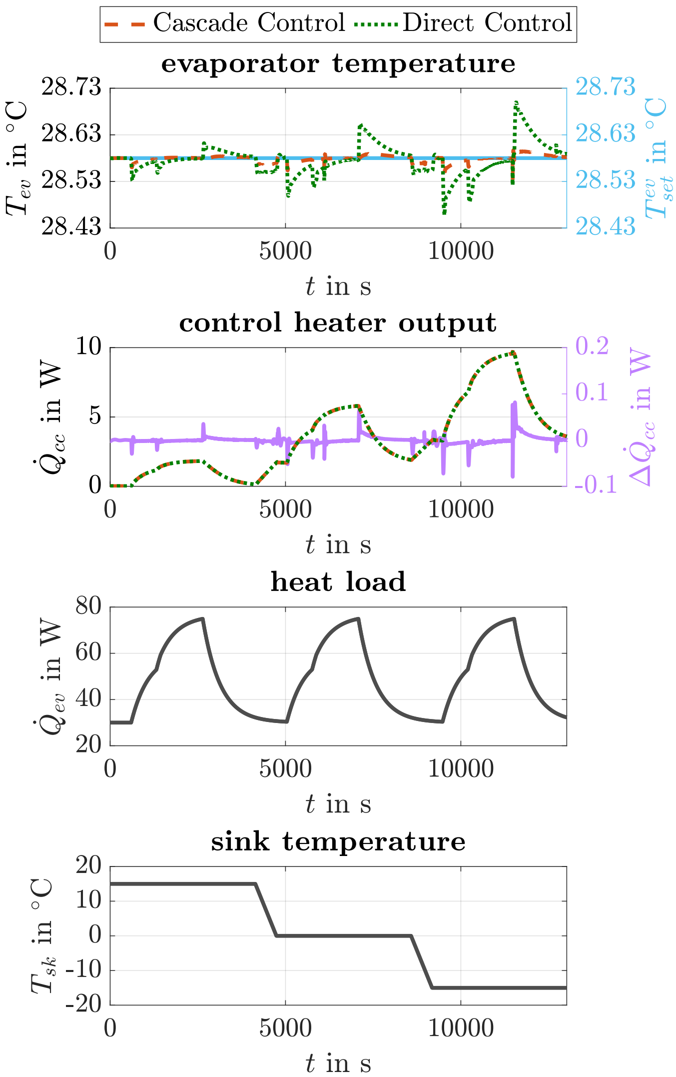

Fig. 3. Disturbance response of the presented cascade control loop in comparison with the direct control loop

Despite the changes of $\dot{Q}_{ev}$ and T_{sk} in the third and forth subplot, both controllers keep T_{ev} near T_{set}^{ev} (solid light blue) in the upper subplot. However, the over- and undershoots in T_{ev} due to the disturbance changes are reduced visibly by the cascade control resulting in an overall smoother T_{ev} than with the direct controller. The improvement of the control performance is emphasized quantitatively by the root mean square error (RMSE) between T_{ev} and T_{set}^{ev} for both controllers, which are RMSE = 0.007 K for the cascade control and RMSE = 0.033 K for the direct controller. Thus, T_{ev} is kept in a smaller corridor by the cascade control as intended.

V. Conclusions

A cascade control for the temperature control of LHPs has been designed based on a dynamical LHP state-space model. By controlling not only the CC temperature, as commonly done in the literature, but also the evaporator temperature as the nearest measurable temperature to the heat source, an improved temperature control performance of the LHP has been achieved compared to the direct control of the evaporator temperature. With the improved LHP temperature control, an improved thermal control of aerospace systems in general is possible. For a complete validation of the proposed LHP controller, its application on a LHP test bench is required in future work. Nevertheless, the simulation results have already shown the promising benefits of the cascade control for LHPs.

References

[1] K. Shukla, “Heat pipe for aerospace applications—an overview,” *Journal of Electronics Cooling and Thermal Control*, vol. 5, no. 1, pp. 1–14, 2015.

[2] J. Ku, “Operating characteristics of loop heat pipes,” in *SAE Technical Paper No. 1999-01-2007*. SAE International, 1999.

[3] ——, “Methods of controlling the loop heat pipe operating temperature,” in *SAE Technical Paper No. 2008-01-1998*. SAE International, 2008.

[4] D. Khrustalev, C. Stouffer, J. Ku, J. Hamilton, and M. Anderson, “Temperature control with two parallel small loop heat pipes for GLM program,” *Frontiers in Heat Pipes*, vol. 5, no. 9, 2014.

[5] J. Ku, K. Paiva, and M. Mantelli, “Loop heat pipe transient behavior using heat source temperature for set point control with thermoelectric converter on reservoir,” in *9th Annual International Energy Conversion Engineering Conference*. American Institute of Aeronautics and Astronautics, 2011.

[6] ——, “Loop heat pipe operation using heat source temperature for set point control,” NASA Technical Reports Server, Tech. Rep. 20110015274, 2011.

[7] T. Gellrich, T. Schuermann, F. Hobus, and S. Hohmann, “Model-based heater control design for loop heat pipes,” in *2nd IEEE Conference on Control Technology and Applications (CCTA)*. IEEE, 2018.

[8] T. Gellrich, S. Meinicke, P. Knipper, S. Hohmann, and T. Wetzel, “Two-degree-of-freedom heater control of a loop heat pipe based on stationary modeling,” in *48th International Conference on Environmental Systems (ICES)*, 2018.

[9] T. Gellrich, X. Zhang, S. Schwab, and S. Hohmann, “Nonlinear model identification adaptive heater control design for loop heat pipes,” in *3rd IEEE Conference on Control Technology and Applications (CCTA)*. IEEE, 2019.

[10] P. Krishnaswamy, G. Rangaiah, R. Jha, and P. Deshpande, “When to use cascade control,” *Industrial & Engineering Chemistry Research*, vol. 29, no. 10, pp. 2163–2166, 1990.

[11] A. Visioli, *Practical PID control*. Springer London, 2006.

[12] MathWorks, *Control system toolbox user’s guide*, The MathWorks, Inc., Natick, Massachusetts, USA, 2020.

[13] S. Meinicke, P. Knipper, C. Helfenritter, and T. Wetzel, “A lean approach of modeling the transient thermal characteristics of loop heat pipes based on experimental investigations,” *Applied Thermal Engineering*, vol. 147, pp. 895–907, 2019.